PROCEEDINGS OF SPIE

SPIEDigitalLibrary.org/conference-proceedings-of-spie

Texture image analysis for osteoporosis detection with morphological tools

Sylvie Sevestre-Ghalila
Amel Benazza-Benyahia
Hichem Cherif
Wided Souid

SPIE.

Texture image analysis for osteoporosis detection with morphological tools

S. Sevestre[a, b], A. Benazza-Benyahia[c], H. Cherif [b], W. Souid[b]

[a] Equipe PRISME, Université Paris V, 45, rue des Saints Pères, 75270 Paris Cedex 06, FRANCE
[b] Laboratoire SYSCOM, Ecole Nationale d'Ingénieurs de Tunis, 1001 Tunis, TUNISIA
[c] Département de Mathématiques Appliquées, Signal et Communications
Ecole Supérieure des Communications de Tunis, 2083 Ariana, TUNISIA

ABSTRACT

The disease of osteoporosis shows itself both in a reduction of the bone mass and a degradation of the microarchitecture of the bone tissue. Radiological images of heel's bone are analyzed in order to extract informations about microarchitectural patterns. We first extract the gray-scale skeleton of the microstructures contained in the underlying images. More precisely, we apply the thinning procedure proposed by Mersal which preserves connectivity of the microarchitecture. Then, a post-processing of the resulting skeleton consists in detecting the points of intersection of the trabecular bones (multiple points). The modified skeleton can be considered as a powerful tool to extract discriminant features between Osteoporotic Patients (OP) and Control Patients (CP). For instance, computing the distance between two horizontal (respectively vertical) adjacent trabecular bones is a straightforward task once the multiple points are available. Statistical tests indicate that the proposed method is more suitable to discriminate between OP and CP than conventional methods based on binary skeleton.

Keywords: Texture, morphology, trabecular bone, osteoporosis detection.

1. INTRODUCTION

Texture analysis is an important problem in image processing because it has an influence on the quality of both image segmentation and interpretation. In this work, we are interested in analyzing the texture contained in radiological images of heel's bone in order to detect the osteoporosis disease. Indeed, the disease of osteoporosis shows itself both in a reduction of the bone mass and a degradation of the microarchitecture of the bone tissue.[1] In this context, since several years, various techniques were developed in order to detect early and efficiently the apparition of this disease.

Concerning the detection of the reduction of bone mass, a noninvasive technique based on Dual-energy X-ray Absorptiometry (DXA) is used.[2] Unfortunately, analyzing the microarchitectures requires until now invasive methods. This is the reason why bone texture analysis operated on radiologic images has recently received a great attention. More precisely, radiographs of heel's bone are very often employed because they contain rich informations on microarchitectural patterns. Furthermore, the underlying image acquisition system can be easily adjusted.[3]

Our approach consists in using morphological tools in order to extract the trabecular bone image. Next, statistical tests are carried out to show that some features of the extracted microstuctures are significantly different between the Osteoporotic Patients (OP) and the Control Patients (CP) and they provide a better discrimination between OP and CP than does the DXA method.

This paper is organized as follows. Section 2 describes the procedure of skeletonization. In section 3, the computation of the relevant features is addressed. Some experimental results and discussion are given in last section.

Further author information: (Send correspondence S. Sevestre-Ghalila)
S. Sevestre-Ghalila E-mail: sevestre@math-info.univ-paris5.fr
A. Benazza-Benyahia E-mail: ben.yahia@planet.tn

Medical Imaging 2001: Image Processing, Milan Sonka, Kenneth M. Hanson, Editors,
Proceedings of SPIE Vol. 4322 (2001) © 2001 SPIE · 1605-7422/01/$15.00

2. COMPUTING THE SKELETON

2.1. Test images

First of all, we give some informations about the acquisition step of the considered images. A mammographic film is used for the formation of each image, the region of interest has a size 2.5 cm $\times$ 2.7 cm. Then, the analog images are digitized with a CCD camera in such manner that a pixel represents an area of 105μm $\times 105\mu$m. Finally, the digital images $I(m,n)$ have a size of 256×256 and they are coded at 8 bpp. Figure 1-(a) shows an example of an OP image and Figure 1-(b) is an example of a CP image.

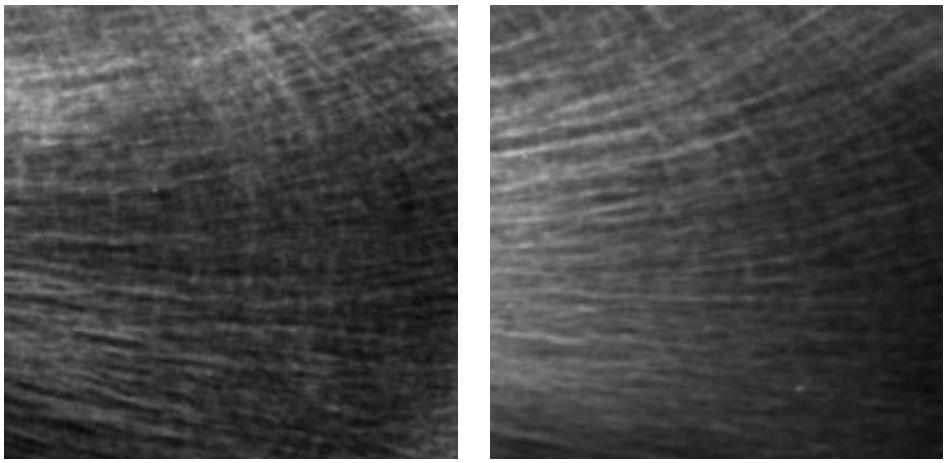

(a) (b)

Figure 1. (a) Heel's bone of an OP, (b) Heel's bone of an CP

2.2. The addressed problem

The aim of the first stage of processing is the extraction of the gray-scale skeleton of the microstructures contained in the underlying images. The gray-scale skeleton consists of the network of arcs which are located along local higher intensity regions.

Although the computation of the skeleton of a binary image is quite straightforward, we do not perform any kind of binarization to avoid to loose an amount of significant information. Indeed, a binarization could affect critically the correctness of the resulting skeleton. In other words, we have to compute the skeleton directly from the original gray-scale image.

But, it is not trivial to define an exact analog of the black-and-white thinning algorithm in the gray-scale case. More precisely, the main problem is the lack of a unifying approach for gray-scale image skeletonization. Several algorithms were developed independently and they do not systematically provide the same results.[4,5]

For the considered application, a meaningful skeleton of the microarchitectures must preserve their connectivity. For this reason, we decide to apply a performant algorithm, recently proposed in[6] and called "new parallel thinning" algorithm.

Before describing this algorithm, some definitions must be given.

2.3. Definitions and notations

The *eight nearest neighbors* of a pixel P are shown in Figure 2. A *path* going from a pixel (k_0, l_0) to a pixel (k_n, l_n) is a sequence of pixels (k_m, l_m) with $1 < m \leq n$ such that pixels (k_m, l_m) and (k_{m-1}, l_{m-1}) are neighbors.

A *hollow* is defined as a connex area of constant intensity k from which any path to pixels not in the region contains pixels having intensity greater than k.

P_7	P_0	P_1
P_6	P	P_2
P_5	P_4	P_3

Figure 2. The eight nearest neighbor of the current pixel P.

A pixel is a *border point* if at least the intensity of P_0, P_2, P_4 or P_6 is zero. Here, we adopt the convention that the zero intensity corresponds to the background and a non-zero intensity is associated with the object (*ie* the trabecular bones).

The connectivity number $CN(P)$ of a pixel P can be expressed as:

$$CN(P) \stackrel{\triangle}{=} \sum_{k=0,2,4,6} (1 - P_k)\&(P_{k+1}||P_{k+2}) \tag{1}$$

where & and || denote respectively the logical "AND" and "OR". Figure 3 shows the different configurations of the neighborhood of a pixel according to the value of its connectivity number.

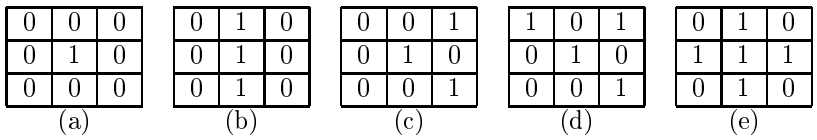

Figure 3. Different configurations for the connectivity number. (a): $CN(P) = 0$, isolated pixel. (b): $CN(P) = 1$, border pixel. (c): $CN(P) = 2$, pixel P connects two sets of pixels. (d): $CN(P) = 3$, branching pixel. (e): $CN(P) = 4$, crossing pixel.

In order to preserve both the connectivity and the salient points of the skeleton, only pixels having a connectivity number less than 1 can be removed.

A pixel is declared *simple* if it suppression does not affect the connectivity number of its neighbors which belong to the object. To identify the simple pixels, the weight number $WN(P)$ of a pixel P has to be defined as:

$$CN(P) \stackrel{\triangle}{=} \sum_{k=0}^{7} 2^k P_k. \tag{2}$$

2.4. The algorithm

The considered algorithm consists of two steps. The first one is a preprocessing step having the objective to suppress the non-significant hollows. Indeed, it is a detection of initial pixels background. The second step builds hollows by growing these starting set of pixels.

1. Preprocessing step
   It first detects pixels considered as edges of the object. Then, the adjacent background pixels are set to hollows. More precisely, it proceeds as follows.
   - A median filtering with a 3×3 sliding window smoothes the image without corrupting its edges.
   - The hollows detection allows to classify the pixels into two groups: the background (class 0) and the object (class 1). This classification is obtained by, first apply the conventional local Sobel filter to evaluate the derivatives $f_x(m,n)$ and $f_y(m,n)$ along respectively the x and y directions, at the current pixel (m,n). Then, the estimate of the gradient magnitude $g(m,n) =\mid f_x(m,n) \mid + \mid f_y(m,n) \mid$ is computed. The pixel (m,n) is classified as an edge pixel if $g(m,n) > \eta$ where the threshold η is computed in order that 10% of

the pixels are classified as edges.
Since the contrast in the image is not uniform, the procedure of edge detection is local. More precisely, the classification is performed within a sliding window of size 32×32. A pixel is visited several times and it assigned to the background if it has detected locally more than 10% of the times.

- A background pixel is then introduced inside the hollow from which the next step of erosion can be initialized.
  The intensity of an edge point is subtracted from those of its 4 nearest neighbors. The amplitude of the neighbor (m_0, n_0) which ensures the maximum absolute difference is set to 0 if $I(m_0, n_0) \leq I(m, n)$. Otherwise, the intensity $I(m, n)$ is set to 0.

2. Iterative procedure of erosion
   Two constraints must be satisfied. First, the connectivity of the hollows must be preserved. Secondly, the connective strength must be maintained. Two kinds of removal (unrestricted and restricted) are iterated in an alternate manner until there is no pixel to be suppressed.

   - The unrestricted suppression attempts to delete the simple pixels P such $CN(P) \leq 1$. The amplitudes of these removed points are sorted in an ascending order and they are stored in a vector $\mathbf{v} = (v_1, v_2, \ldots, v_n)$.
   - The restricted removal consists in suppressing the border points P which are simple with a $CN(P) \leq 1$ and which have an intensity not greater than v_1, then not greater than v_2 and so on until v_n. By taking into account the gray levels in the image, the restricted suppression aims to make uniform the hollow.

In this way, the trabecular bones (*ie* to the morphological contents of the image) are extracted. This thinning procedure is homotopic which is a crucial property for shape description applications. Rosenfeld *et al.* proved that any thinning algorithm which takes into account the simple pixels preserves the connectivity of the original image.[7] Furthermore, another salient advantage is its low computational cost since only comparisons and shifts are carried out.

The iterations are order $o(256^2)$. To reduce the execution time, it is possible to implement the algorithm according to a parallel architecture. Figure 4 shows the resulting skeleton. It corresponds to a connected network.

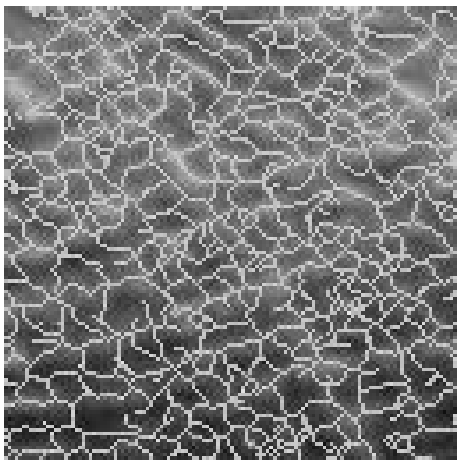

Figure 4. Resulting skeleton of an OP.

3. EXTRACTING SOMME DISCRIMINANT FEATURES

The obtained skeleton has to be exploited in order to caracterize quantitatively the texture of the heel's bone. Precisely, we are interesting here in quantify the morphological aspect of the skeleton.

So we propose first to evaluate the skeleton length to quantify the thickness of the trabecular bone. Secondly, to quantify the disconnection of trabecular bone, we compute the number of points of the network.

Finally, we choose to estimate the distances between two adjacent trabecular bones because it is an important feature which characterizes the microarchitecture of the bone. Indeed, we compute the distances between two adjacent intersection points of the skeleton. These ones can be viewed as the multiple points of the skeleton and they can easily be extracted from a 4-connected network.[8] Therefore, a thinning procedure is applied on the 8-connected skeleton in order to obtain a 4-connected network. More precisely, within a sliding window 2×2, the pixels of the skeleton having the minimal connectivity number are suppressed without altering the connectivity of the initial skeleton. Then, a second postprocessing step consisting in detecting the points of intersection of the network is applied. The objective is to locate the branching points or the crossing points (see Figure 3-(d),(e)). So, the resulting skeleton is depicted in Figure 5. It has a one-pixel thin and the multiple points (enlighted points) correspond to the intersections of the trabecular bones.

At this level, the skeleton can be exploited to extract discriminant features between OP and CP. More precisely, we

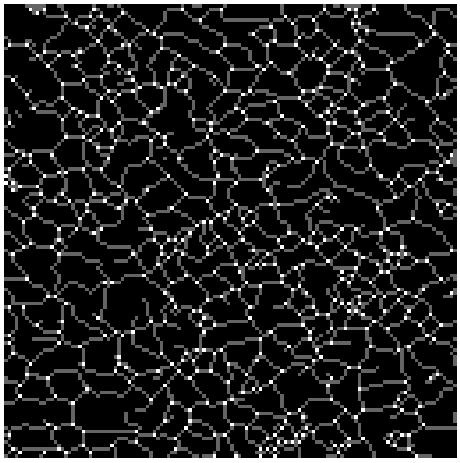

Figure 5. Post-processed skeleton of an OP, the enlighted points represent the multiple points.

propose to determine the length of the skeleton, the distances between two adjacent multiple points and the ending point. For these latter features, their extraction is performed according to the horizontal and the vertical directions in order to take into account the bidirectionality of the trabecular network. More precisely, the horizontal (resp. vertical) "distance" d_h (resp. d_v) gives the number of pixels separating two successive multiple points when the starting pixel of the arc connecting them may be located, first, at the neighbors P_1, P_2 and P_3.

The ending point e_h (resp. e_v) are detected from a multiple points as the same manner as trabecular distances.

4. EXPERIMENTAL RESULTS

A number of 36 images of osteoporosis patient and 38 images of control patients are avalaible.

To enligth our contribution, we compare the discriminant ability of the resulting gray-scale skeleton with the discriminant ability of the binary skeleton. The latter can be obtain, from a binary version of the original image which is derived by applying a 5×5 sliding window on the original gray image and within the mask, the pixels smaller than the median are set to 0. Once the binary image is avalaible, the morphological skeletonization described by P. Soille[8] is used. The process is illustrated at figure 4-(a),(b),(c).

To compare the resulting binary and gray-scale skeletons gives a first visually knowledge about the capacity of the gray-scale skeleton for extracting the trabecular network from the image. The example of the figure 4 enligths lot of trabecular bone no detected by the binary but detected by the gray-scale approach. Table 1 also provides the performances of the two kinds of skeleton. The table 1 shows that all selected features have a discriminant power. Globally, we can see that the results of the white test are better for the gray-scale skeleton except for the number of horizontal ending points and the length of the skeleton.

The fist one is the number of ending points in the horizontal direction but the p-value are very closed. Both binary and gray-scale skeletons give approximately the same p-value.

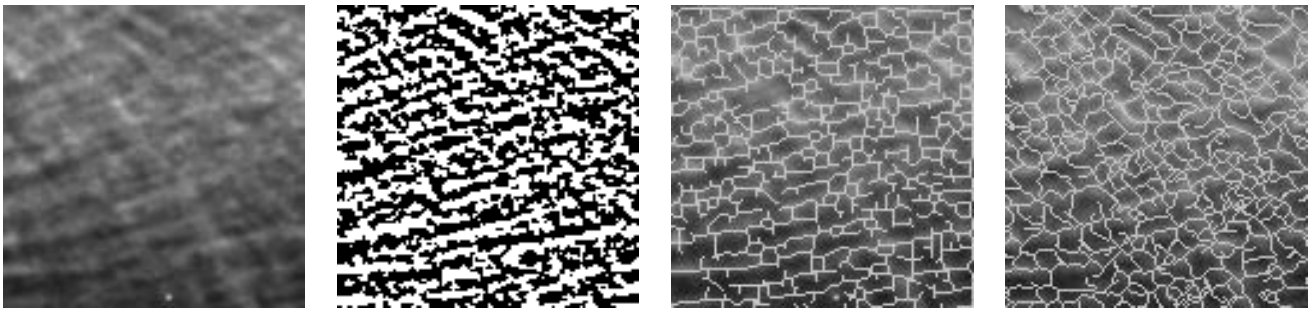

(a) (b) (c) (d)

Figure 6. (a) Heel's bone of an OP, (b) Binary version of (a) obtained by applying a 5×5 sliding window on (a) and within the mask, the pixels smaller than the median are set to 0 (c) Binary skeleton of (b), (d) gray-scale skeleton of (a)

Table 1. Statistical results of discriminant ability of 5 features: number of ending points on vertical and horizontal directions, length of the skeleton and trabecular distance on vertical and horizontal directions. For each feature, this table gives the first(q_1) et the third quartile (q_3), the mean and the standart deviation of the distribution on each sample image OP and CP. The p-value of White test is used to detect the difference of the feature on the two test sets.

Features	OP : [q1, q3] (mean ± StD)	CP : [q1, q3] (mean ± StD)	White test p-value
Number of ending points H	[1082, 1151] (1115 ± 77)	[1048, 1119] (1079 ± 62)	cp<op 0.008
Number of ending points V	[674, 749] (711 ± 65)	[623, 709] (671 ± 59)	cp<op 0.0039
Length of the network (pixel)	[48065, 48708] (48429 ± 936)	[48337, 49379] (48973 ± 812)	cp>op 0.0023
Trabecular Distances H	[3.74, 3.86] (3.8 ± 0.08)	[3.77, 3.89] (3.84 ± 0.09)	cp>op 0.066
Trabecular Distances V	[4.12, 4.33] (4.27 ± 0.23)	[4.2, 4.47] (4.39 ± 0.25)	cp>op 0.005

(a) Gray skeleton

Features	OP : [q1, q3] (mean ± StD)	CP : [q1, q3] (mean ± StD)	White test p-value
Number of ending points H	[1148, 1294] (1224 ± 102)	[1092, 1201] (1157 ± 76)	cp<op 0.0032
Number of ending points V	[673, 816] (757 ± 93)	[649, 743] (702 ± 74)	cp<op 0.0101
Length of the network (pixel)	[14583, 15363] (14979 ± 603)	[14172, 14816] (1454 ± 448)	cp<op 7.88 10-4
Trabecular Distances H	[4.22, 4.71] (4.51 ± 0.4)	[4.28, 4.87] (4.68 ± 0.53)	cp>op 0.0746
Tabecular Distances V	[6.03, 7.13] (6.58 ± 0.6)	[6.32, 7.11] (6.83 ± 0.59)	cp>op 0.0674

(b) Binary skeleton

The second is the length of the skeleton. For binary skeleton, the white test decides that the length is greater for OP than for CP. The opposite conclusion holds from the gray-scale skeleton. In fact, the trabecular bone of an OP is degraded by the disease. Therefore OP image should have a "smaller" skeleton than an CP image. And this property is well enlighted by the white test operated on the gray-scale skeleton is used.

Finally, it is worth to study the correlation existing between the different features we proposed to extract. The empirical correlation matrix of 5 considered feature vector (Tabecular Distances H, Tabecular Distances V, Number of pixels in network, Number of ending points H, Number of ending points V) given in the following indicates that

some redundancies exist among these features:

$$\begin{pmatrix} 1.0000 & 0.4226 & 0.4224 & -0.4607 & -0.3798 \\ 0.4226 & 1.0000 & 0.9124 & -0.8485 & -0.8618 \\ 0.4224 & 0.9124 & 1.0000 & -0.9127 & -0.8894 \\ -0.4607 & -0.8485 & -0.9127 & 1.0000 & 0.7884 \\ -0.3798 & -0.8618 & -0.8894 & 0.7884 & 1.0000 \end{pmatrix}$$

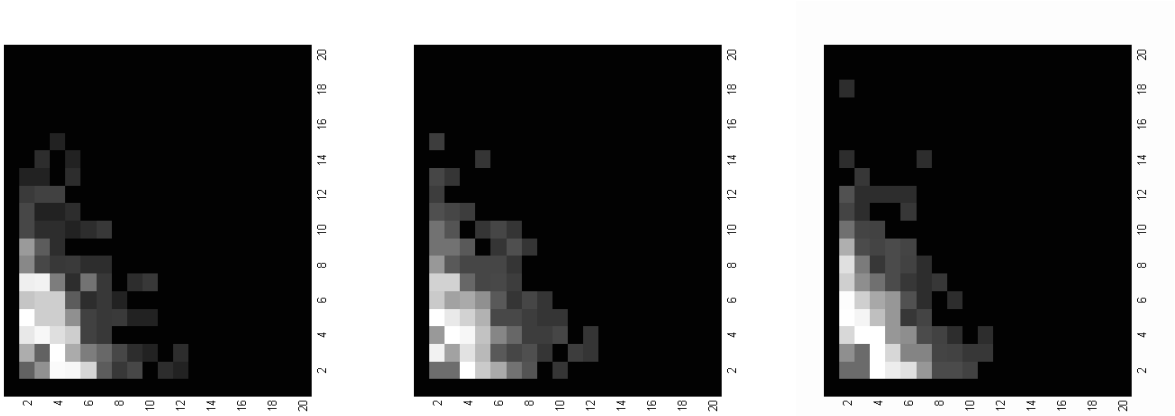

(a) Control patients

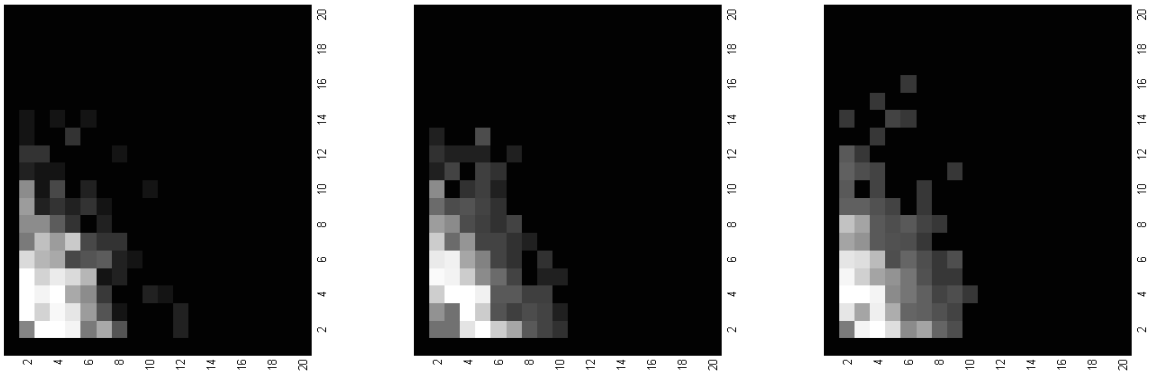

(b) Osteoporotic patients

Figure 7. Histogram of the distances (d_h, d_v) for some test images by using gray-scale skeleton.

Therefore, it would be more suitable to incorporate an additional information or another feature. Preliminary simulations carried out on twenty images that the dynamic of the histogram of the distances (d_h, d_v) allows to classify between OP and CP. Indeed figure 7 show that this dynamic seems to be larger for OP than for CP.

In conclusion, the gray-scale skeleton is a suitable tool for extracting morphological information on microarchitecture than binary version.

ACKNOWLEDGMENTS

The authors thanks Dr C. L. Benhamou and his team of CHR Orleans La Source (France) for offering to analyse the texture of thier images studied in this paper. The authors also radiology service of Charles Nicolle Hospital of Tunis (Tunisia) for having financial supported this work.

REFERENCES

1. C.L. Benhamou, E. Lespessailles, V. Royant, "Architecture osseuse et résistance mécanique du tissu osseux," *la Presse Médicale*, **25**, No. 6, pp. 249-254, 1996.
2. S. Grampp, H.K. Genant, A. Mathur, P. Lang, M. Jergas, M. Takada *et al.*, "Comparisons of noninvasive bone mineral measurements in assessing age-related loss, fracture discrimination and diagnostic classification," *JBMR*, **12**, pp. 697-711, 1997.
3. C.L. Benhamou, E. Lespessailles, V. Royant, " Fractal organisation of trabecular bone images on calcaneus radiographs," *JBMR*, **9**, No. 12, pp. 1909-1918, 1994.
4. C. Arcelli, G. Ramella, "Finding grey skeletons by iterated pixel removal," *Image and Vision Computing*, **13**, No. 3, pp. 159-267, April 1995.
5. S. Chen, F. Shih, "Skeletonization for fuzzy degraded character images," *IEEE Trans. on Image Processing*, **5**, No. 10, pp. 1481-1485, October 1996.
6. S. S. Mersal, A.M. Darwish, "A new parallel thinning algorithm for gray scale images," IEEE Nonlinear Signal and Image Processing Conference,*NSIP'99*, Antalya, Turkey, June 1999.
7. A. Rosenfeld, L.S. Davis, "A note on thinning", *IEEE Trans. on System Man Cybernetics*, SMC-6, no. 3, pp. 226-228, 1976.
8. P. Soille, "Morphological Image Analysis". Principles and Applications", Springer-Verlag, 1999.